Subpicosecond thin-disk laser oscillator with pulse energies of up to 25.9 microjoules by use of an active multipass geometry

Joerg Neuhaus[1,2,*], Dominik Bauer[1,2], Jing Zhang[1], Alexander Killi[2], Jochen Kleinbauer[2], Malte Kumkar[2,3], Sascha Weiler[2], Mircea Guina[4], Dirk H. Sutter[2], and Thomas Dekorsy[1]

[1]*Department of Physics and Center of Applied Photonics, University of Konstanz, 78457 Konstanz, Germany*

[2]*TRUMPF-Laser GmbH + Co. KG, Aichhalder Str. 39, 78713 Schramberg, Germany*

[3]*JT Optical Engine GmbH + Co. KG, Prüssingstr. 41, 07745 Jena, Germany*

[4]*Tampere University of Technology, Korkeakoulunkatu 3, 33720 Tampere, Finlandand RefleKron Ltd., Muotialankuja 5 C5, Tampere 33800, Finland*

joerg.neuhaus@uni-konstanz.de

Abstract: The pulse shaping dynamics of a diode-pumped laser oscillator with active multipass cell was studied experimentally and numerically. We demonstrate the generation of high energy subpicosecond pulses with a pulse energy of up to 25.9 μJ at a pulse duration of 928 fs directly from a thin-disk laser oscillator. These results are achieved by employing a selfimaging active multipass geometry operated in ambient atmosphere. Stable single pulse operation has been obtained with an average output power in excess of 76 W and at a repetition rate of 2.93 MHz. Self starting passive mode locking was accomplished using a semiconductor saturable absorber mirror. The experimental results are compared with numerical simulations, showing good agreement including the appearance of Kelly sidebands. Furthermore, a modified soliton-area theorem for approximating the pulse duration is presented.

OCIS codes: (140.3480) Lasers, diode-pumped; (140.3580) Lasers, solid-state; (140.4050) Mode-locked lasers

References and links

1. B. N. Chichkov, C. Momma, S. Nolte, F. von Alvensleben, and A. Tünnermann, "Femtosecond, picosecond and nanosecond laser ablation of solids," Appl. Phys. A **63**, 109–115 (1996).
2. F. Brunner, E. Innerhofer, S. V. Marchese, T. Südmeyer, R. Paschotta, T. Usami, H. Ito, S. Kurimura, K. Kitamura, G. Arisholm, and U. Keller, "Powerful red-green-blue laser source pumped with a mode-locked thin disk laser," Opt. Lett. **29**, 1921 (2004).
3. L. Shah, M. E. Fermann, J. W. Dawson, and C. P. J. Barty, "Micromachining with a 50W, 50 μJ, subpicosecond fiber laser system," Opt. Express **14**, 12,546–12,551 (2006).

#101765 - $15.00 USD Received 22 Sep 2008; revised 30 Oct 2008; accepted 11 Nov 2008; published 26 Nov 2008

4. P. Baum and A. H. Zewail, "Attosecond electron pulses for 4D diffraction and microscopy," PNAS **104**, 409–414 (2007).
5. S. V. Marchese, C. R. Baer, A. G. Engqvist, S. Hashimoto, D. J. Maas, M. Golling, T. Südmeyer, and U. Keller, "Femtosecond thin disk laser oscillator with pulse energy beyond the 10-microjoule level," Opt. Express **16**, 6397 (2008).
6. F. Röser, D. Schimpf, B. Ortac, K. Rademaker, J. Limpert, and A. Tünnermann, "90W average power 100μJ energy femtosecond fiber chirped-pulse amplification system," Opt. Lett. **32**, 2230–2232 (2007).
7. S. Naumov, A. Fernandez, R. Graf, P. Dombi, F. Krausz, and A. Apolonski, "Approaching the microjoule frontier with femtosecond laser oscillators," New J. Phys. **7**, 216 (2005).
8. S. Dewald, T. Lang, C. D. Schröter, R. Moshammer, J. Ullrich, M. Siegel, and U. Morgner, "Ionization of noble gases with pulses directly from a laser oscillator," Opt. Lett. **31**, 2072 (2006).
9. A. Killi, A. Steinmann, J. Dörring, U. Morgner, M. J. Lederer, D. Kopf, and C. Fallnich, "High-peak-power pulses from a cavity-dumped Yb:KY$(WO_4)_2$ oscillator," Opt. Lett. **30**, 1891–1893 (2005).
10. G. Palmer, M. Emons, M. Siegel, A. Steinmann, M. Schultze, M. J. Lederer, and U. Morgner, "Passively mode-locked and cavity-dumped Yb : KY$(WO_4)_2$ oscillator with positive dispersion," Opt. Express **15**, 16017–16021 (2007).
11. E. Innerhofer, T. Südmeyer, F. Brunner, R. Häring, A. Aschwanden, R. Paschotta, C. Hönninger, M. Kumkar, and U. Keller, "60W average power in 810fs pulses from a thin-disk Yb:YAG laser," Opt. Lett. **28**, 367 (2003).
12. S. V. Marchese, T. Südmeyer, M. Golling, R. Grange, and U. Keller, "Pulse energy scaling to 5μJ from a femtosecond thin disk laser," Opt. Lett. **31**, 2728 (2006).
13. A. Giesen, H. Hügel, A. Voss, K. Wittig, U. Brauch, and H. Opower, "Scalable concept for diode-pumped high-power solid-state lasers," Appl. Phys. B **58**, 365–372 (1994).
14. A. M. Scott, G. Cook, and A. P. G. Davies, "Efficient high-gain laser amplification from a low-gain amplifier by use of self-imaging multipass geometry," Appl. Opt. **40**, 2461 (2001).
15. M. Kumkar, "Laser Amplification System," U.S. Pat. 6765947, U.S. Pat. (2006).
16. J. Neuhaus, J. Kleinbauer, A. Killi, S. Weiler, D. H. Sutter, and T. Dekorsy, "Passively mode-locked Yb:YAG thin-disk laser with pulse energies exceeding 13μJ by use of an active multipass geometry," Opt. Lett. **33**, 726–729 (2008).
17. U. Keller, K. J. Weingarten, F. X. Kärtner, D. Kopf, B. Braun, I. D. Jung, R. Fluck, C. Hönninger, N. Matuschek, and J. Aus der Au, "Semiconductor saturable absorber mirrors (SESAMs) for femtosecond to nanosecond pulse generation in solid-state lasers," IEEE J. Sel. Top. Quantum Electron. **2**, 435, (1996).
18. F. X. Kärtner, I. D. Jung, and U. Keller, "Soliton mode-locking with saturable absorbers," IEEE J. Sel. Top. Quantum Electron. **2**, 540–556 (1996).
19. E. T. J. Nibbering, G. Grillon, M. A. Franco, B. S. Prade, and A. Mysyrowicz, "Determination of the inertial contribution to the nonlinear refractive index of air, N_2 , and O_2 by use of unfocused high-intensity femtosecond laser pulses," J. Opt. Soc. Am. B **14**, 650 (1997).
20. M. Haiml, R. Grange, and U. Keller, "Optical characterization of semiconductor saturable absorbers," Appl. Phys. B **79**, 331–339 (2004).
21. F. X. Kärtner and U. Keller, "Stabilization of soliton like pulses with a slow saturable absorber," Opt. Lett. **20**, 16 (1995).
22. C. Hönninger, R. Paschotta, F. Morier-Genoud, M. Moser, and U. Keller, "Q-switching stability limits of continuous-wave passive mode locking," J. Opt. Soc. Am. B **16**, 46–56 (1999).
23. F. X. Kärtner, J. Aus der Au, and U. Keller, "Mode-Locking with Slow and Fast Saturable Absorbers - What's the Difference?" IEEE J. Sel. Top. Quantum Electron. **4**, 159 (1998).
24. S. M. Kelly, "Characteristic sideband instability of periodically amplified average soliton," Electron. Lett. **28**, 806–807 (1992).

1. Introduction

Ultrashort laser pulses in the microjoule regime are of prime importance for many applications, including high-speed micromachining [1], pumping of optical parametric oscillators and amplifiers, as well as basic research, e.g. in high-field physics or for the generation of attosecond electron pulses [2, 3, 4, 5]. As compared to external amplifiers [3, 6], ultrafast oscillators are very attractive due to their simplicity and compactness. To some extend the pulse energies from an oscillator can be increased by using extended resonator cavities [5, 7, 8] or by cavity dumping [9, 10]. Previous maximum pulse energies obtained directly from an oscillator in ambient atmosphere were below 2μJ. These pulse energies were limited by the strong self-phase modulation (SPM) of air [11]. Higher pulse energies were obtained in a He-flooded cavity with pulse energies of 5.1μJ [12] and 11μJ [5] at subpicosecond pulse lengths. One way to de-

#101765 - $15.00 USD Received 22 Sep 2008; revised 30 Oct 2008; accepted 11 Nov 2008; published 26 Nov 2008

crease the SPM is to use larger output-coupling (OC) rates in combination with a high-gain medium. In order to reach high average powers together with high pulse energies a thin-disk (TD) laser crystal is the medium of choice [13], allowing for power scalability by increasing the beam size and exploiting the excellent cooling properties of the TD. However, the low gain of a TD laser has to be overcome. Therefore, we have increased the round trip gain by passing the gain medium successively under different angles within one round trip by use of a novel active multipass cell (AMC). This approach has previously been used in laser amplifiers with conventional solid-state rod geometries [14], as well as in thin-disk amplifiers [15]. Recently we have obtained pulse energies of 13.4 μJ with an active multipass cell operated in air [16]. Here, we report on the generation of pulse energies of up to 25.9 μJ in ambient atmosphere by increasing the pump-spot size on the TD and by the use of different semiconductor saturable absorber mirrors (SESAMs) [17].

2. Experimental results with an active multipass geometry

Experiments have been performed with 11 and 13 passes through an AMC. Whereas the experiments with 13 passes were done for a further increase of the pulse energy, a more detailed analysis at various pump powers and by use of different SESAMs was accomplished for the laser operating with 11 passes through the AMC.

At a repetition rate of 3.4 MHz, corresponding to 11 passes through the AMC — or 44 passes through the gain medium —, a pulse energy of up to 20 μJ at a maximum average output power of 68 W was obtained. The laser was operated at a total pump power of 219 W and an OC rate of $\approx 64\%$. A pulse duration of 811 fs, deduced from the autocorrelation assuming an ideal sech^2 shape, and a spectral bandwidth of 1.48 nm (FWHM) at a center wavelength of 1030 nm was measured. The resulting time bandwidth product of 0.34 is within 10% of the transform limit of 0.315 for soliton pulses.

The experimental setup of the laser is shown in Fig. 1. The telescopic mirrors (M2 and M7) had a focal length of 1.25 m. Six dispersive mirrors were included in the AMC design with a total GDD of $-0.18\,\mathrm{ps}^2$ per cavity round trip. The dispersive mirrors had a reflectivity of about 99.85% and > 132 bounces within each round trip. The Yb:YAG disk had a thickness of $60\mu m$ and a wedge angle of 0.1°. The pumping chamber provided 20 passes through the gain medium, leading to an estimated absorption of less than 73% for the fiber-coupled 940 nm pump power. The estimation was done by a numerical simulation that simulated rate equations between gain, laser power, and pump power. The optical to optical efficiency was 31%, whereas when taking into account the anticipated amount of pump absorption an effective optical to optical efficiency can be calculated to be 42%.

While in the experiments described here the same pump chamber and TD as in Ref. [16] was used, in contrast to Ref. [16] the laser was operated at a larger spot size on the TD (1 mm in radius), in order to minimize thermal lensing and to increase the maximum possible pump power without risking damage of the disk. The CW background as observed in Ref. [16] at wavelengths far off the peak wavelength of the pulses was found to be enlarged for small mode radii or imprecise overlap of the various modes on the TD. A precise adjustment of the mode radii with respect to the pump mode size is especially difficult for a large dioptric power of the TD, which was observed for a small pump spot size and large pump powers as described in Ref. [16]. By using a larger pump spot width (1 mm) the dioptric power of the TD was mostly eliminated. Hence, better control of the mode radii was possible and the CW background was completely suppressed for all pump powers.

The high round trip gain allowed for output-coupling (OC) rates of up to 78% (with 13 passes through the AMC), which is - to our knowledge - the highest OC rate of any TD laser reported so far. Thereby the ratio of intracavity pulse energy to external energy was greatly reduced,

#101765 - $15.00 USD Received 22 Sep 2008; revised 30 Oct 2008; accepted 11 Nov 2008; published 26 Nov 2008

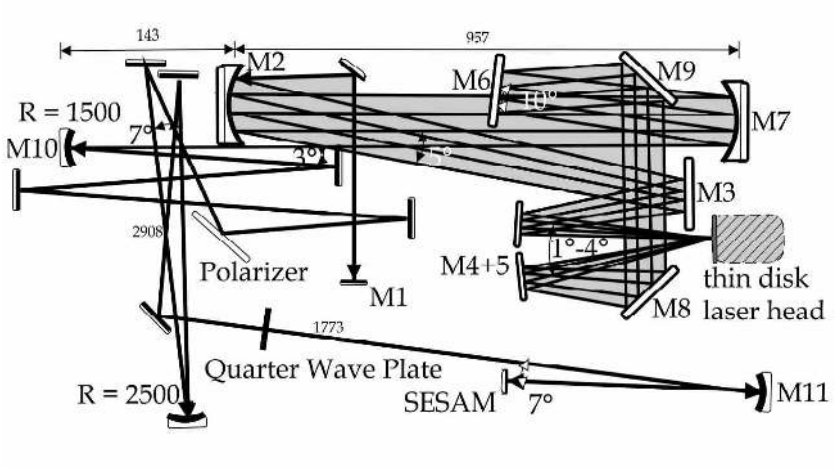

Fig. 1. Schematic design of the passively mode-locked Yb:YAG thin-disk laser with angular multiplexing. For reasons of clarity, in this figure only four passes through the AMC have been plotted. The actual experimental setup contained 11 or 13 passes through the AMC with a total cavity length of 44 m for 11 passes and 51 m for 13 passes. Six dispersive mirrors were included in the AMC design with a total GDD of $-0.180\,\mathrm{ps}^2$ per cavity round trip for 11 passes through the AMC, respectively. The quarter wave plate allowed for arbitrary OC rates. The lengths given specify the distance in between two arrows in millimeters, therefore possibly including some bounces over plan mirrors. Furthermore the radius of curvature for every concave mirror is also given in millimeters.

such that helium flooding could be avoided. Strong SPM balanced by large negative group delay dispersion (GDD) resulted in soliton mode locking as the predominant pulse shaping mechanism [18]. The B-integral per round trip was calculated to be $B = 0.9\,\mathrm{rad}$ (for $32\,\mu\mathrm{J}$ pulses before OC) at maximum, mainly originating from the nonlinear refractive index of air. For a Gaussian beam, the SPM-coefficient can be calculated according to

$$\gamma_{\mathrm{SPM}} = \frac{4n_2}{\lambda}\int \frac{dz}{w^2}, \tag{1}$$

with n_2 being the nonlinear refractive index of the material and w the spot size at the respective position. It was found that for the resonator cavity used in this work the SPM coefficient caused by air can be calculated for a Gaussian beam by using the formula

$$\gamma_{\mathrm{SPM}} \approx N_{\mathrm{img}} \cdot \frac{4n_2}{\lambda} \cdot \frac{\pi^2}{\lambda}. \tag{2}$$

Here, N_{img} is the number of passes through the AMC plus the number of telescopic arrangements, e.g. $4f$ imaging arrangements, outside of the AMC and a respective fraction for the remaining part of the cavity, alltogether taken twice for one complete round trip. This formula is independent of the mode size on the TD and the actual focal length of the mirrors in the AMC; consequently, it can be used for easily calculating the SPM coefficient for different number of passes through the AMC. With a nonlinear refractive index of air of $4.0 \cdot 10^{-23}\,\mathrm{m}^2/\mathrm{W}$ [19], a total SPM coefficient of $\approx 37.5 \cdot 10^{-3}\,\mathrm{MW}^{-1}$ was calculated ($N_{\mathrm{img,ext}} = 1.4$ for the part outside the AMC); the contribution caused by the TD is smaller than 2%. Dispersive mirrors introduced a total GDD of $-0.1787\,\mathrm{ps}^2$ per round trip including the positive dispersion introduced by the gain medium.

#101765 - $15.00 USD Received 22 Sep 2008; revised 30 Oct 2008; accepted 11 Nov 2008; published 26 Nov 2008

The beam profile measured at maximum output power with a commercial camera-based system was close to diffraction limited (an $M^2 < 1.3$ was measured for the largest external pulse energies at a micromachining setup behind an acousto-optic modulator).

Passive mode locking of the laser was started and stabilized with the help of a SESAM [17]. In contrast to the experiments in Ref. [16] a larger mode radius of $450\,\mu$m was chosen on the SESAM. Operation at even larger spot sizes was unstable, due to a nonspherical curvature of the SESAM surface; the chosen spot size still leads to a strong saturation ($F/F_{\mathrm{sat}} \approx 65$, with F and F_{sat} being the fluence and saturation fluence, respectively) at the maximum internal pulse energy of approximately $32\,\mu$J ($20\,\mu$J external pulse energy). The mode size was controlled with a camera-based system. Due to a remaining slight thermal lens dioptric power, partly caused by the highly dispersive chirped mirrors (HDCMs), the mode size on the SESAM decreased to a minimum of $400\,\mu$m for smaller internal pulse energies with less pump power. As a result, Q-switched mode locking (QML) was further suppressed as compared to the case without any change in mode size on the SESAM. No degradation of the SESAM (or any other optical component) was observed during several hours of operation.

Experiments with 11 passes through the AMC have been performed with four different SESAMs; the SESAMs were characterized by using a pump-probe setup with 80 fs pulses at 1030 nm and pulse fluences, similar to those in the laser cavity. The reflectivity curve of the SESAM was fitted with a macroscopic model function as given by [20]:

$$R(F) = R_{\mathrm{ns}} \frac{\ln\left(1 + R_{\mathrm{lin}}/R_{\mathrm{ns}} \cdot (\exp(F/F_{\mathrm{sat}}) - 1)\right)}{F/F_{\mathrm{sat}}} \exp\left(\frac{-F}{F_2}\right), \tag{3}$$

resulting in the parameters as listed in Tab. 1. R_{lin} is the linear reflectivity of the unsaturated SESAM, R_{ns} the nonsaturable loss in absence of two-photon absorption (TPA), and F_2 is the rollover coefficient, attributed to TPA for the pulses used in the pump-probe setup. The modulation depth of the SESAM is then given by $\Delta R = R_{\mathrm{lin}} - R_{\mathrm{ns}}$. The SESAMs had a fast relaxation time of some hundred femtoseconds and a slow relaxation component with a relaxation time of some tens of picoseconds. The results of the experiments with 11 passes through the AMC at various pump powers are listed in Tab. 2, whereas only the parameters for the experiments with the highest energy available for single pulse operation are shown for each specific SESAM, with exception of additional experiments at lower pump powers for operation with SAM-B1. The amplitude noise was measured by using the statistics function of the oscillscope that was used. The respective root mean square (RMS) noise as listed in Tab. 2 is given by the standard deviation of the area below the oscilloscope trace within a time window encompassing one complete pulse trace; measured over a respectable number of pulses, it includes high and also very low frequency noise components. Operation with SAM-R1 and SAM-R2 showed a much larger RMS noise, partly caused by operation closer to the critical energy for QML as a result of the larger modulation depth, and due to a different mounting procedure (SAM-R1 and SAM-R2 were mounted on a copper plate by use of silver conductive paste) that is presumably more sensitive to thermal effects.

The relationship between GDD, SPM, external pulse energy, and pulse length was independent of the actual SESAM that was used. When assuming an exponential increase of the pulse energy inside the resonator an average intracavity pulse energy can be calculated. In combination with the soliton area theorem [21, 18] a modified soliton area theorem for a laser comprising an AMC can then be found:

$$\tau_P \approx \frac{-1.76 \cdot 2|\beta_2| \ln(1 - OC)}{\gamma_{\mathrm{SPM}} E_{P,\mathrm{ext}}}. \tag{4}$$

Here, β_2 is the total GDD per round trip, γ_{SPM} the SPM coefficient, OC the output coupling

#101765 - $15.00 USD Received 22 Sep 2008; revised 30 Oct 2008; accepted 11 Nov 2008; published 26 Nov 2008

rate, and $E_{P,\mathrm{ext}}$ the external pulse energy of the resonator. The pulse length over energy according to this modified version of the soliton area theorem is plotted in Fig. 2 together with the measured pulse durations over external pulse energy for all experiments with 11 passes through the AMC and an OC rate of 64%. Hence, soliton mode locking was confirmed by the applicability of this modified version of the soliton area theorem.

SESAM	SAM-B1	SAM-B2	SAM-R1	SAM-R2
Bragg Mirror	GaAs/AlAs	GaAs/AlAs	GaAs/AlAs	GaAs/AlAs
QW-Material	InGaAs	InGaAs	InGaAsN	InGaAs
design	A-FPSA	A-FPSA	A-FPSA	A-FPSA
ΔR	0.84%	0.5%	3.5%	2.6%
$F_{\mathrm{sat}}(\mu\mathrm{J/cm}^2)$	35	22	61	32
$F_2(\mathrm{J/cm}^2)$	291	0.126	0.108	0.106

Table 1. Parameters of the SESAMs, used in the mode locking experiments.

QML and double pulsing was observed for operation with all SESAMs at very large and small pump powers; thereby setting a lower and upper limit, respectively, for stable mode locking. The range of operation for each SESAM is highlighted in Fig. 2. Whereas QML is mostly influenced by the modulation depth and the saturation fluence [22] the onset of double pulsing is affected only by the modulation depth of the SESAM [23]. A large modulation depth should prevent double pulsing. However, for pulses in the picosecond regime ($> 1\,\mathrm{ps}$) small modulation depths of the SESAM were sufficient, whereas for subpicosecond pulses double pulses could only be suppressed by use of SESAMs with larger modulation depths, as can be seen from the results of the experiments shown in Fig. 2.

Operation with SAM-B1, having a small modulation depth and therefore only a small tendency for QML, showed a large stable continuous-wave mode locking (CWML) operation range, which can be seen in Fig. 3. In the figure, the output power is plotted over the pump power, whereas the pump powers leading to the occurence of double pulses and QML are highlighted. The results for this specific SESAM at various pump powers are shown here in more detail. SAM-B1 was already used in the experiments described in Ref. [16] to initiate and stabilize mode locking.

	$P^{(P)}(\mathrm{W})$	$P^{(L)}(\mathrm{W})$	$E_P(\mu\mathrm{J})$	$\Delta\lambda(\mathrm{nm})$	$\tau_{\mathrm{FWHM}}(\mathrm{fs})$	TBP	RMS
SAM-R1	219	68.3	20.1	1.48	811	0.34	7%
SAM-R2	193	63	18.6	1.22	953	0.33	10%
SAM-B1	165	55	16.2	1.08	1086	0.33	2%
SAM-B2	160	52	15.3	0.88	1228	0.31	1%
SAM-B1	151	48	14.1	0.96	1255	0.34	2%
SAM-B1	130	38	11.1	0.74	1536	0.32	1%
SAM-B1	109	29	8.4	0.55	2000	0.31	1%
SAM-B1	88	20	6	0.37	3110	0.33	1%
SAM-B1	67	13	3.8	0.23	5274	0.34	1%

Table 2. Results of the mode-locking experiments with various SESAMs and 11 passes through the AMC. For SAM-B1 the resulting parameters for experiments at varying pump powers are listed, whereas for the experiments with the other three SESAMs, only those measurements that resulted in stable CWML just before the onset of double pulsing are shown.

#101765 - $15.00 USD Received 22 Sep 2008; revised 30 Oct 2008; accepted 11 Nov 2008; published 26 Nov 2008

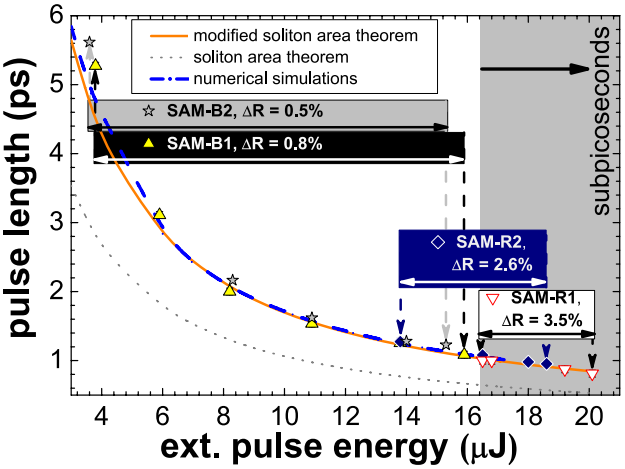

Fig. 2. Pulse length over pulse energy for experiments with 11 passes through the AMC at various pump powers and for operation with different SESAMs, showing a reciprocal dependence of the pulse width on the pulse energy. The range of stable CWML is highlighted for each SESAM by a coloured bar (grey, black, blue, and white) and the smallest and largest pulse energies, at which stable mode locking was observed, are each marked by a vertical arrow. For pulse energies lower than the specified range QML was observed, whereas the upper limit was set by the onset of double pulsing. The pulse length as expected from a modified soliton area theorem is also included in this figure, as well as the results given by numerical simulations that simulate the evolution of the electric field inside the laser cavity.

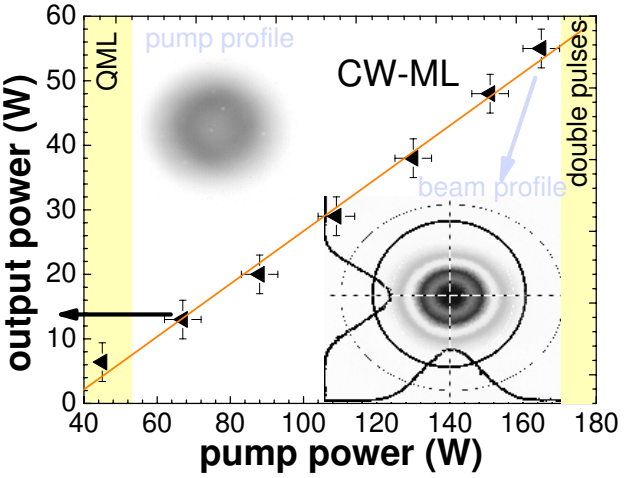

Fig. 3. Output power for the experiments with SAM-B1. Operation with the occurrence of QML and double pulses is highlighted. The left inset shows a profile of the pump spot, whereas the right inset shows the laser mode, as measured with a camera based system just before the SESAM, for operation with the largest pulse energies.

#101765 - $15.00 USD Received 22 Sep 2008; revised 30 Oct 2008; accepted 11 Nov 2008; published 26 Nov 2008

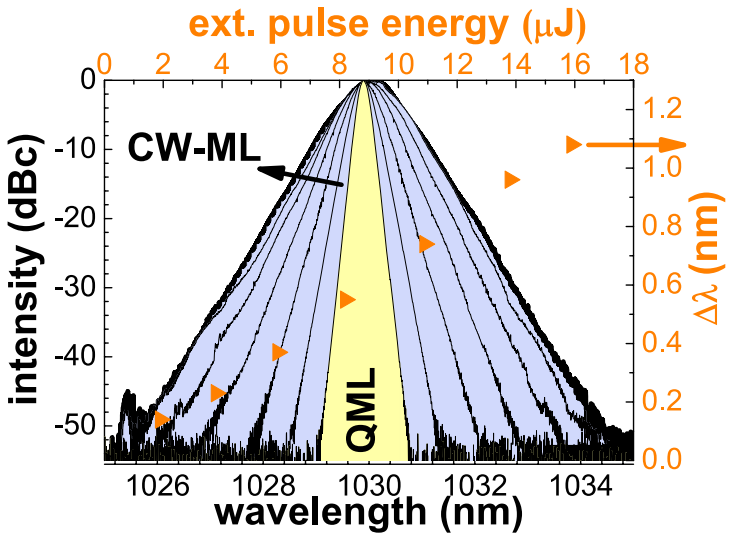

Fig. 4. Optical spectra for the experiments with SAM-B1 at various pump powers from 67 W to 165 W as listed in Tab. 2. The optical bandwidth is indicated at the right axis, assuming an ideal sech^2 fit of the optical spectrum.

With SAM-B1 a maximum pulse energy of 16.2 μJ at a pulse length of 1086 fs and an average output power of 55 W was obtained before double pulses were observed. As can be seen in Fig. 4, the spectral bandwidth was 1.08 nm at a center wavelength of 1030.1 nm, resulting in a TBP of 0.33, which is within 10% of the transform limit of 0.315 for soliton pulses. A total B-integral per round trip of 0.56 rad was estimated. The beam profile for stable CWML at the largest pump power is shown in the inset of Fig. 3.

Despite the large number of passes through the TD the resonator was not only stable over the full range of pump powers but even allowed for nearly diffraction-limited operation and stable ML for most of this range, due to the negligible change of thermal lens dioptric power of the disk, caused by the larger diameter of the pump spot as compared to the experiments in Ref. [16]. The larger pump spot, requiring a larger laser mode, is the reason for an increase in the critical energy according to the QML criterion. Hence, in contrast to the experiments described in Ref. [16], for pump powers below 55 W, QML rather than CW operation was observed.

Increasing the number of passes through the AMC towards 13, i.e. 52 passes through the gain medium, a maximum average output power of 76 W was obtained at a total pump power of 236W and an OC rate of 78%. At a repetition rate of 2.93 MHz this corresponds to a pulse energy of 25.9 μJ. The spectrum measured at this pulse energy is shown in Fig. 5 and the autocorrelation trace is shown in Fig. 6. A pulse duration of 928 fs, deduced from the autocorrelation assuming an ideal sech^2 shape, and a spectral bandwidth of 1.22 nm (FWHM) at a center wavelength of 1030 nm was measured. The resulting time bandwidth product of 0.32 is within 10% of the transform limit of 0.315 for soliton pulses. For mode locking the laser SAM-R1 was used. Different to the experiments with 11 passes through the AMC, Kelly sidebands [24] were visible at the outer sides of the spectrum. They are caused by an increased total GDD due to the additional passes through the AMC. Within the figure also the spectrum as given by numerical simulations is shown, showing Kelly sidebands at the respective positions. In order to adjust the position of the Kelly sidebands, the GDD and third order dispersion (TOD) were used as fit parameters, resulting in a total GDD of $-0.193\,\mathrm{ps}^2$ and a TOD of $-0.00226\,\mathrm{ps}^3$. The width of the spectrum was further adjusted by using the pulse energy as fit parameter, resulting in a pulse energy of 24.52 μJ. With an SPM coefficient of $44.45 \cdot 10^{-9}\,\mathrm{MW}^{-1}$, the resulting pulse length according to Eq. (4) would be 943 fs, whereas the simulations resulted in a pulse length

#101765 - $15.00 USD Received 22 Sep 2008; revised 30 Oct 2008; accepted 11 Nov 2008; published 26 Nov 2008

of 938 fs. Both are in good agreement with the experimentally obtained pulse duration.

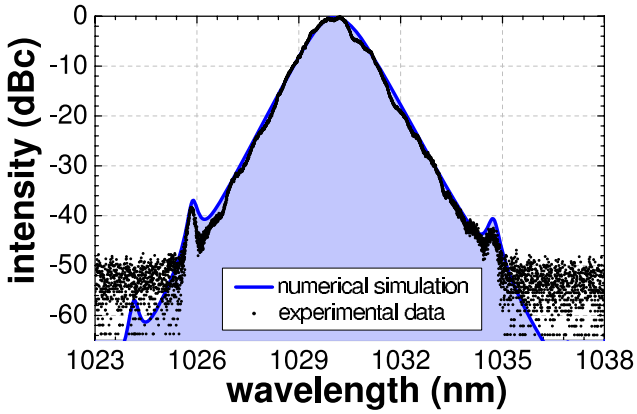

Fig. 5. Spectrum of experiment with 13 passes through the AMC. Kelly sidebands are clearly visible, agreeing well with the position of the Kelly sidebands as anticipated from the numerical simulation. In the numerical simulation (blue line), however, only GDD was included.

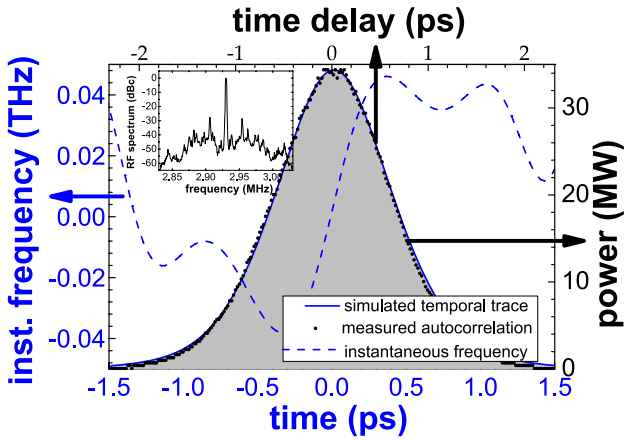

Fig. 6. Pulse trace in the time domain (black solid line) and the instantaneous frequency (dashed blue line) as given by numerical simulation of the experiment with 13 passes through the AMC. The inset shows the measured rf-spectrum, showing sidebands which are about 25 kHz apart from the carrier frequency. The amplitude of these sidebands was strongly dependent on the flow rate of the cooling mechanism of the TD, however without shifting in position.

3. Result and conclusion

In conclusion, we have demonstrated a subpicosecond laser oscillator producing pulse energies beyond the 20 μJ level without external amplification. The laser was operated in ambient atmosphere. Pulse energies of up to 25.9 μJ have been obtained with an unamplified solid-state laser oscillator comprising an AMC within the laser cavity. We presented detailed experimental results on this laser architecture, which appears to be the least complex for generating high

#101765 - $15.00 USD Received 22 Sep 2008; revised 30 Oct 2008; accepted 11 Nov 2008; published 26 Nov 2008

energy pulses directly from an oscillator. The concept allowed for (i) an easy alignment of the components, (ii) enough GDD by only few dispersive mirrors to compensate for the SPM due to air, (iii) enough gain to overcome cavity losses, (iv) a high OC and thus low intracavity pulse energies, and (v) a large gain bandwidth for the generation of subpicosecond pulses. A modified version of the soliton area theorem was presented for approximating the relationship between external pulse energy, GDD, SPM, and pulse length of a laser oscillator with AMC and large output-coupling rate.

Even higher pulse energies can be obtained by increasing the resonator length further, e.g. by introducing an additional passive multipass cell into the laser resonator. However, the experiments were not limited by the pump-power density at the moment, which can be increased by using more passes of the pump light over the TD, increasing the pump absorption from $\approx 74\%$ to 100%, or by using a pump diode with larger output power. Instead, the obtained pulse energies were limited by the onset of double pulsing. The occurrence of multiple pulsing can be most likely attributed to the decreased modulation depth of the SESAMs caused by TPA.

This work was partly funded by the German Federal Ministry of Education and Research, contract 13N8580 and by a grant from the Ministry of Science, Research and the Arts of Baden-Württemberg. We thank J. Demsar, M. Beyer, and H. Schäfer for access to the pump-probe setup.

#101765 - $15.00 USD Received 22 Sep 2008; revised 30 Oct 2008; accepted 11 Nov 2008; published 26 Nov 2008